Chem. Chem. Technol., 2025,
Vol. 19, No. 2, pp. 183–195

Chemistry

EFFECT OF PHYSICO-CHEMICAL MODIFICATION OF CLINOPTILOLITE COMPOSITES ON THEIR ANTIMICROBIAL ACTIVITY

Volodymyr Vasylechko[1,2], Volodymyr Sydorchuk[3], Nazar Manko[4,✉], Oksana Kostiv[1], Ol'ga Klyuchivska[4], Oleksandra Ilkov[5], Svitlana Bagday[1], Anatoliy Zelinskiy[1], Oleksandr Gromyko[6], Rostyslav Stoika[4], Yaroslav Kalychak[1]

https://doi.org/10.23939/chcht19.02.183

Abstract. Microparticles based on natural Transcarpathian clinoptilolite (CL), its H- and Na-forms are synthesized by physicochemical modifications, in particular, heat treatment and doping with metal activators (Ag and Cu). Doping of CL samples with metal ions was carried out in two different ways: the first was to use the solid-phase extraction method under dynamic conditions followed by mechanochemical treatment, and the second was to mechanochemically treat the CL samples with Ag and Cu compounds. XRD, SEM, EDX, FTIR-, UV-Vis-, XPS spectra, dispersity, porous structure parameters and antibacterial activity of the obtained compositions were studied. Modified forms are characterized by increased dispersion, larger specific surface area, porosity, increased number of hydroxyl OH groups and siloxane bonds. The inclusion of metals in the structure of CL contributed to the formation of active red-ox centers responsible for the formation of active oxygen-containing particles that participate in the destruction of microorganisms, which significantly increases the antibacterial activity of CL. The physical stability and biotolerance of CL in connection with the proposed approaches of physicochemical modification of zeolite will be useful for the preparation of new agents for the disinfection of contaminated surfaces in industry, agriculture, *etc.*

Keywords: clinoptilolite, microparticles, transition metals, physico-chemical and mechanochemical modifications, antimicrobial action.

1. Introduction

Decontamination of surfaces remains an urgent problem, especially during hostilities and in the war and post-war periods. Today, this problem is mainly solved with the help of agents containing chlorine compounds, organic and peroxo compounds[1]. However, such sterilization methods have numerous disadvantages. During the chemical interaction of reagents of the disinfectants with the organic compounds present on surfaces or with the organic materials of different surfaces, toxic substances can be formed. The latter get into the wash water and, furtherly, especially in field conditions, can appear in natural ecosystems, harming the environment. The use of chlorinated lime can lead to corrosion of metallic products, and, therefore, to a failure of equipment, inventory, weapons, and military equipment.

In recent decades, there has been a growing interest in the study of antimicrobial, sorption and catalytic properties of solid nanomaterials, in particular natural zeolites[2–6]. Zeolite compositions, in particular the "clinoptilolite - Ag^{+}" compositions, were proposed for the disposal of combat toxic chemical substances of nerve-paralytic action (VX, zarin) and bacteriological agents[2–4].

A successful use of natural zeolites as biologically active materials requires the study of their physicochemical properties, namely the nature of their surface, porosity, structure, adsorption capacity, and other characteristics. Activation of the biological action of zeolite materials can be carried out using thermal and chemical treatment, for example, with acid, replacement of cations in the exchange complex, their doping with cations of certain metals, as well as a mechanochemical modification using various micronization approaches[7, 8].

[1] Faculty of Chemistry, Ivan Franko National University of Lviv, 6, Kyryla & Mefodiya str., Lviv, 79005, Ukraine
[2] Department of Food Technology, Lviv University of Trade and Economics, 9, Samchuka str., Lviv, 79011, Ukraine
[3] Department of Heterogeneous Catalytic Oxidation Processes, Institute of Sorption and Problems of Endoecology, NAS of Ukraine, 13, General Naumov str., Kyiv, 03164, Ukraine
[4] Department of Regulation of Cell Proliferation and Apoptosis, Institute of Cell Biology, NAS of Ukraine, 14/16, Drahomanov str., Lviv, 79005, Ukraine
[5] Halychpharm, 6, Opryshkivska str., Lviv, 79024, Ukraine
[6] Faculty of Biology, Ivan Franko National University of Lviv, 4, Hrushevskoho str., Lviv, 79005, Ukraine
✉ *mankonazarcb@gmail.com*

Clinoptilolite is the most common natural zeolite[9, 10]. This mineral belongs to the heylandite group and has a generalized formula $(K_2Na_2Ca)_3[Al_6Si_{30}O_{72}]\cdot 24H_2O$. CL is a biologically neutral and non-toxic zeolite[7]. It is the only representative of natural zeolites approved for use in medical practice and food industry[7, 11–13].

In previous studies, we and other authors[14–22] found a powerful antimicrobial effect of the CL–Ag^+ and CL–Cu^{2+} compositions, as well as the anticancer and immunomodulatory effects of the CL–Ag^+ composition. Since Ag^+ and Cu^{2+} ions can interact with sulfhydryl groups (R–SH) present in proteins, it is believed that the antibacterial activity of cations of these transition metals, in particular during their stay in the zeolite matrix, is proportionally dependent on their affinity for sulfur-containing groups[23].

This study aimed to develop efficient approaches for structure-functional modification of the microparticles (MPs) of Transcarpathian clinoptilolite (CL) *via* their mechanochemical, thermal and chemical (doping with Ag and Cu cations) treatments. The final goal of such modifications was to enhance the antimicrobial action of these zeolite materials to be used for the inactivation of bacteria or fungi and the degradation of dangerous chemical pollutants.

2. Experimental

2.1. Materials and Reagents

CL from the deposit of Sokyrnytsia of the Transcarpathian region (Ukraine) was used in this research. The mineral contained 85–90 % (wt.) of the main component. The dominant impurity is alpha quartz. The formula of the Transcarpathian CL in the oxide version (wt. %) is as following: SiO_2 – 67.29; TiO_2 – 0.26; Al_2O_3 – 12.32; Fe_2O_3 – 1.26; FeO – 0.25; MgO – 0.99; CaO – 3.01; Na_2O – 0.66; K_2O – 2.76; H_2O – 10.90[24]. Transcarpathian CL belongs to the low-silica calcium variety of CL and does not contain clay impurities.[24] Its specific surface, determined by water, is 59 $m^2\cdot g^{-1}$ [25]. The zeolite samples were ground in an agate mortar with an agate pestle, and a fraction of grains of 0.20–0.31 mm size was taken, washed with distilled water, and dried at room temperature.

The zeolite samples were ground in a mortar with a pestle, and a fraction of grains of the required size was taken, washed with distilled water, and dried at room temperature.

Some samples of CL were calcined at the appropriate temperature for 2.5 h in a drying oven WSU200 (VEB MLW, Germany) and a muffle furnace SNOL 7.2/1100 (AB Utenos Elektrotechnika, Lithuania). After heat treatment, the zeolite samples were cooled to a temperature of 20 ± 1ºC in a desiccator.

H-form of CL was obtained *via* treatment with HNO_3, following the literature data[26]. The ground CL (6 g) was pre-treated with 200 mL of a 1.0 M HNO_3 solution for 24 h at a temperature of 20 ± 1 °C. After separation from the acid solution, the obtained H-form of CL was washed in distilled water and dried at room temperature.

When obtaining the Na-form of CL (Na-CL), we used a partially modified technique described in[27]. The powder of CL was preconditioned with a 0.25 M HNO_3 solution for 4 h at room temperature. Then, the zeolite fraction was separated, washed with distilled water, and treated with a 1 M $NaNO_3$ solution for 1–1.5 h (repeated 7–8 times). The obtained Na-clinoptilolite was dried at room temperature.

All used reagents were of analytical grade. The bidistilled water was used to prepare the reagent solutions. The standard solutions of Ag(I) and Cu(II) (1.0 mg mL^{-1}) were obtained *via* dissolving of $AgNO_3$ and $Cu(NO_3)_2$. The content of Ag(I) and Cu(II) was determined titrimetrically. The required pH value of the working solutions was created by adding dilute solutions (~0.005 M) of NaOH or HNO_3.

2.2. Preparation of Samples Doped with Ag^+ and Cu^{2+} Ions by Sorption and Mechanochemical Modification

The preparation of samples of various forms of CL doped with Ag^+ and Cu^{2+} ions was carried out under dynamic conditions in the solid-phase extraction mode. It was used for this peristaltic pump NP-101 (RDD BIPH, Ukraine). The methods of investigation performed under dynamic conditions were described in detail elsewhere[28].

A spectrophotometric method with the use of sulfarsazen was used to control the moment of Ag^+ slippage. The optical density of the solutions was measured at λ = 540 nm. Control of the Cu^{2+} slip moment was also carried out spectrophotometrically (spectrophotometer Ulab 102, Shanghai Metash Instruments Co., Ltd., China) using 1-(2-pyridylazo)-2-naphthol (PAN), measuring the optical density of the solutions at λ = 540 nm.

The content of Ag^+ and Cu^{2+} in solutions and eluates was determined by the atomic absorption method on an atomic absorption spectrophotometer C-115 M1 (Selmi, Ukraine) in the flame version (propane – butane – air). The wavelength of the resonance radiation during the measurement of the silver and copper concentrations was 328.1 and 324.8 nm, respectively.

When choosing the conditions for the preparation of "CL – Ag^+" samples, the data described in[14], "CL – Cu^{2+}"[25], "H-CL – Ag^+"[15], "Na-CL – Ag^+"[16] were partially used. All samples "CL – Ag^+", "CL – Cu^{2+}", "H-CL – Ag^+" and "Na-CL – Ag^+" obtained using the method of

solid-phase extraction were subjected to MChT (rotation speed – 400 rpm, treatment duration – 1 h).

Silver nitrate and metallic silver powder were used as dopants in the mechanochemical modification. The source of copper was copper (II) nitrate trihydrate, copper (I) oxide, and copper metal powder.

Preparation conditions and characteristics of the samples are given in Table 1.

Table 1. List of samples of natural CL and compositions based on it

No. sample	Form of CL*	Method of obtaining the forms of CL	Pretreatment temperature of CL, ºC	The method of obtaining a sample**	Dopant
	CL		–	–	–
	H-CL	1 M HNO_3	–	–	–
9	CL	–	–	MChT	$AgNO_3$ (2 mg $Ag \cdot g^{-1}$)
13	CL	–	550	MChT	$AgNO_3$ (10 mg $Ag \cdot g^{-1}$)
15	CL	–	160	MChT	$Cu(NO_3)_2$ (3 mg $Cu \cdot g^{-1}$)
17	Na-CL	1 M $NaNO_3$	–	MChT	–
18	Na-CL	1 M $NaNO_3$	–	MChT	$AgNO_3$ (2 mg $Ag \cdot g^{-1}$)
19	H-CL	1 M HNO_3	–	MChT	–
20	H-CL	1 M HNO_3	–	MChT	$AgNO_3$ (2 mg $Ag \cdot g^{-1}$)
21	CL	–	350	MChT	–
22	CL	–	350	MChT	$AgNO_3$ (2 mg $Ag \cdot g^{-1}$)
23	CL	–	–	sorption	$AgNO_3$ (2 mg $Ag \cdot g^{-1}$)
24	CL	–	350	sorption	$AgNO_3$ (2 mg $Ag \cdot g^{-1}$)
25	CL	–	550	sorption	$AgNO_3$ (10 mg $Ag \cdot g^{-1}$)
26	CL	–	160	sorption	$Cu(NO_3)_2$ (3 mg $Cu \cdot g^{-1}$)
27	Na-CL	1 M $NaNO_3$	–	sorption	$AgNO_3$ (2 mg $Ag \cdot g^{-1}$)
28	Na-CL	1 M $NaNO_3$	–	sorption	$AgNO_3$ (6 mg $Ag \cdot g^{-1}$)
29	H-CL	1 M HNO_3	–	sorption	$AgNO_3$ (2 mg $Ag \cdot g^{-1}$)
30	H-CL	1 M HNO_3	–	sorption	$AgNO_3$ (6 mg $Ag \cdot g^{-1}$)
31	CL	–	160	sorption	$Cu(NO_3)_2$ (0,65 mg $Cu \cdot g^{-1}$)
36	CL	–	160	–	–
37	CL	–	550	MChT	–
38	CL	–	–	MChT	–
39	CL			MChT	$AgNO_3$ (1 mg $Ag \cdot g^{-1}$)
40	CL	–	–	MChT	$AgNO_3$ (2 mg $Ag \cdot g^{-1}$)
41	CL	–	–	MChT	Cu_2O (3 mg $Cu \cdot g^{-1}$)
42	CL	–	–	MChT	Cu metal
43	CL	–	–	MChT	Ag metal
45	H-CL	1 M HNO_3	–	MChT	$AgNO_3$ (1 mg $Ag \cdot g^{-1}$)
46	H-CL	1 M HNO_3	–	MChT	$AgNO_3$ (6 mg $Ag \cdot g^{-1}$)
47	CL	–	550	MChT	$AgNO_3$ (6 mg $Ag \cdot g^{-1}$)

* CL – natural clinoptilolite, H-CL-acid modified form of clinoptilolite, Na-CL-sodium modified form of clinoptilolite.
** The samples obtained by sorption were subjected to MChT after the sorption process.

2.3. X-Ray Diffraction and Scanning Electron Microscope Investigation

Diffraction data were obtained on a powder diffractometer STOE STADI P (STOE & Cie GmbH, Germany) (Cu $K\alpha_1$-radiation, $\lambda = 1.54060$ Å, $2.500 \leq 2\theta \leq 90.325°$, step scan mode with a step size 0.015° and a counting time of 100–250 s per data point). Structural characteristics are calculated using *WinCSD* program package[29].

Morphology of the studied samples was investigated using a scanning electron microscope (SEM) TESCAN Vega3 LMU (TESCAN, Czech Republic). Quantitative composition of the samples was studied using energy-dispersive X-ray analyzer (EDX) (Oxford Instruments, UK).

2.4. Mechanochemical Treatment

Natural clinoptilolite, its calcined, as well as H- and Na-forms were subjected to milling (mechanochemical treatment) in air (dry MChT) at 300–500 rpm for 0.5–2.5 h (cycles of 15 min with a pause of 5 min and reverse) using a planetary ball mill "Pulverisette-6" (Fritsch, Germany) with a Si_3N_4 vessel. 12 balls with a diameter of

20 mm from Si_3N_4 (were used as grinding bodies). The mass of the sample was 5 g.

2.5. Particle Size Distribution

The particle size distribution was evaluated using a Mastersizer 2000 laser diffraction analyzer (Malvern Ins., UK). Water dispersions of powders were used.

2.6. Low-Temperature Nitrogen Adsorption-Desorption Isotherms

The parameters of porous structure were calculated from isotherms of low-temperature nitrogen adsorption-desorption which were measured using analyzer NOVA 2200 (Quantachrome, USA) after outgassing of samples at 150 ^{0}C for 20 h. Specific surface area S, micropores volume V_{mi}, mesopores volume V_{me} were determined using BET, BJH and t-methods, respectively. Sorption pore volume V_s was determined at a relative pressure of nitrogen about 0.99. Volume of macropores with size in the range 50–200 nm V_{ma} was calculated from isotherms using adsorption value at relative pressure in the range 0.963–0.99[30]. Mesopores size d was determined from pore size distribution (PSD) curves plotted using desorption branches of the isotherms.

2.7. FTIR Spectroscopy

FTIR spectra were recorded using the "Spectrum-One" spectrometer (Perkin-Elmer Instruments, USA) in the reflection mode. Sample to KBr ratio in the powder mixture was 1:20. The spectra were recorded without preliminary dehydration of the powders.

2.8. UV-Vis Spectroscopy

Electronic spectra of diffuse reflection were measured in the wavelength range of 200–800 nm. For this, a Lambda 35 UV-Vis spectrophotometer (Labsphere RSA-PE-20 attachment) was used (Perkin – Elmer Instruments, USA).

2.9. XPS Spectroscopy

The selected samples have been studied using X-ray photoelectron spectroscopy (XPS) which was previously used to determine the state of small amounts of transition metals in carbon and zeolite matrices[31, 32]. UHV-Analysis System produced by SPECS Surface Nano Analysis Company (Germany) was used for XPS spectra acquisition and a Mg K source (h = 1253.6 eV) was employed for spectra excitation, which was measured at constant pass energy of 35 eV. The charge drift was compensated using the 1s line of adventitious carbon by setting its binding energy (BE) to 284.6 eV.

2.10. Measurement of Antibacterial Activity

The antibacterial effect was determined using the MTT reagent. The strains of used bacteria are: *Staphylococcus aureus* ATCC25923, *Bacillus subtilis* ATCC31324, *Pseudomonas aeruginosa* ATCC9027, *Pseudomonas fluorescens* IMB8573. All strains were taken from Microorganisms Collection of Biololgy Faculty of Ivan Franko National University. The bacterial culture in the logarithmic phase of growth in Sabouraud's medium, pH 7.2, was centrifuged for 10 min at 500 g, and the bacterial sediment was washed with sterile physiological solution and resuspended. A defined volume of this suspension was injected into Sabouraud's medium to achieve an optical density (OD) of 0.4–0.6 at 590 nm (optical path 1.0 cm). 100 μL of each bacterial suspension was injected into Eppendorf tubes (2 mL), and then, inoculated with the test sample CL. Each experiment was repeated three times. The test tubes were incubated for 4 h at 37 ºC. Then, 10 μL of solution (5 mg·mL^{-1}) of the MTT reagent (3-(4,5-dimethylthiazol-2-yl)-2,5-diphenyltetrazolium bromide), Sigma, USA) was introduced and the incubation was continued for 1 h. Cells were collected by centrifugation for 5 min at 1.500 g, the supernatant was removed by centrifugation, and the sediment was suspended in 1 ml of dimethylsulfoxide (DMSO). After incubation for 1 h at 37 ºC, the optical density of the liquid was measured at 580 nm on a ULAB 102 UV spectrophotometer (Ukraine).

2.11. Statistical Analysis

Antibacterial data were presented as the mean (M) ± standard deviation (SD). Results were analysed and illustrated with GraphPad Prism (version 10; GraphPad Software, San Diego, CA, USA). Statistical analyses were performed using two-way ANOVA with Dunnett's multiple comparisons test (cells growth inhibition). A P-value of <0.05 was considered as statistically significant.

3. Results and Discussion

The diffractogram of natural CL contains diffraction reflections from CL and alpha-quartz and is shown in Fig. 1, *a*. The refined lattice constants are: a=17.654(2), b=17.943(3), c=7.4025(9) Å, β=116.345(6)° for CL and a=4.9163(8), c=5.407(7) Å for α-SiO_2 and are in good agreement with literature data[32]. The H-CL diffractogram is similar to the previous one, but the intensities of some reflexes are different that are related to cation exchange. The lattice constants: a=17.657(2), b=17.964(3), c=7.4063(6)Å, β=116.325(5) slightly differ from those in the natural form.

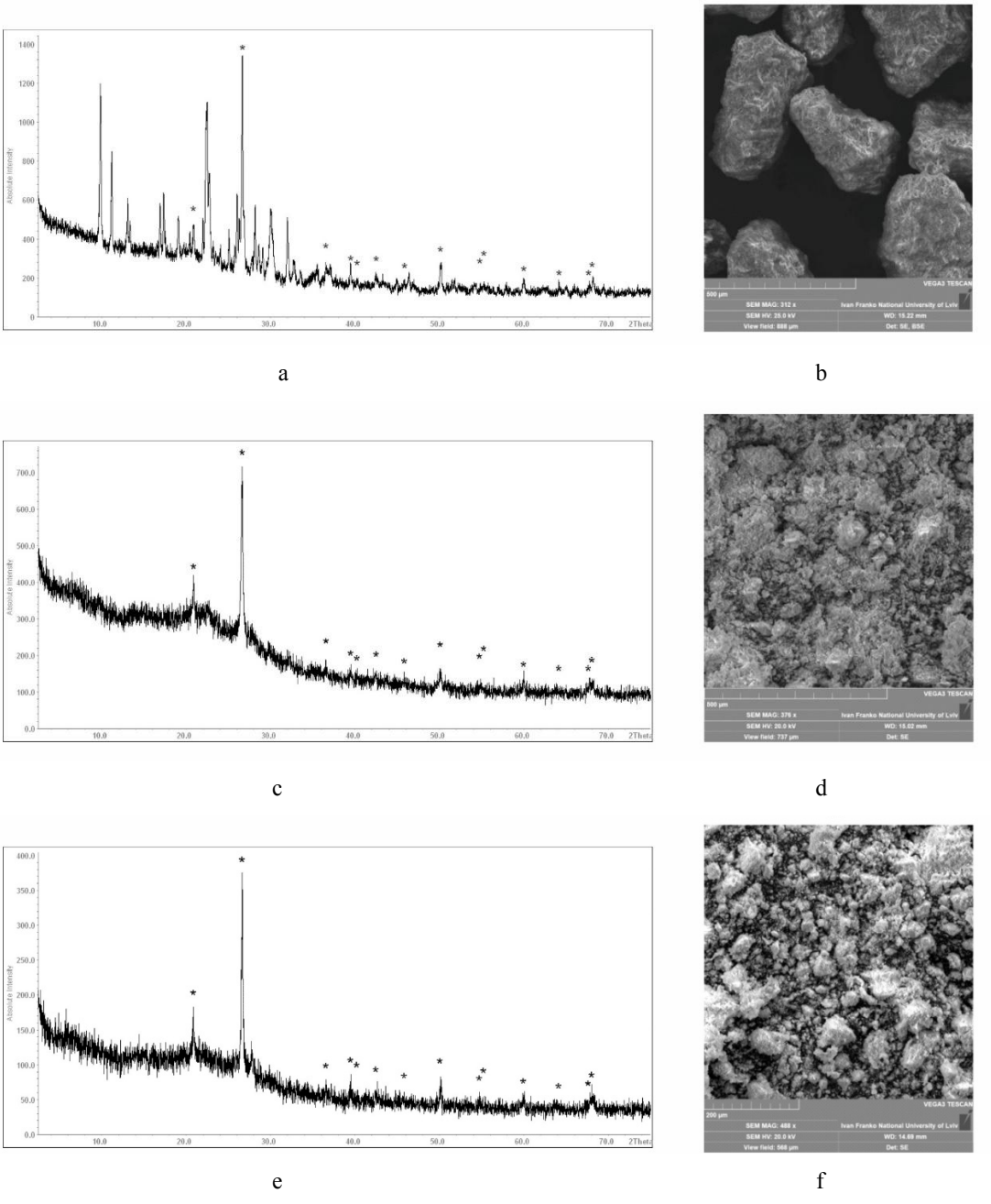

Fig. 1. Diffraction pattern of natural CL (**a**), the samples after milling (**c** – No. 22, **e** – No. 29) and SEM image of natural CL (**b**), the samples after milling (**d** – No. 22, **f** – No. 29). Asterisks indicate peaks from the concomitant α-quartz phase

The MChT of natural and modified forms of CL in a high-energy mill leads to the gradual destruction (amorphization) of the crystalline structure of CL. The degree of destruction depends on the intensity of the MChT, time and environment in which the grinding is carried out, and the temperature of the preliminary heat treatment of CL. Dry milling promotes greater destruction than processing in liquid media, which correlates well with data[32]. The destruction is accompanied by a decrease in the intensities of the reflections from CL and an increase in the intensity of the halo on the diffractogram, which characterizes the content of the amorphous phase. More intense and long-lasting MChT – the diffraction peaks from CL disappeared completely and the crystalline phase remained impurity alpha-quartz. Preliminary heat treatment of the CL facilitates the destruction of its structure during a subsequent MChT. For example, Fig. 1, *c* and *e*, respectively, present the diffractograms of the

samples obtained by MChT during 1 h at 400 rpm and by sorption from a solution followed by grinding under the same conditions. Clinoptilolite phase is in an amorphized state.

The results of scanning electron microscopy of natural CL suggest its granular structure. Granules are isolated, slightly elongated and have sizes in the range of 200–500 μm (Fig. 1, *b*). The H-form of natural CL also has a similar morphology. The samples after MChT consist of particles of different sizes and shapes: they are disoriented and gather into agglomerates (Fig. 1, *d*, *f*). As the intensity and time of grinding increased, the number of smaller particles increased too.

3.1. Characteristics of the Porous Structure of CL Particles

Natural CL is a micro-mesoporous material[30, 33–35]. However, cations Na, K, Ca, located in narrow channels, block micropores, which practically do not contribute to the sorption volume of pores. Therefore, the obtained nitrogen adsorption-desorption isotherms (Fig. 2, *a*) can belong to mixed type II and IV (or type IIb) isotherms with a hysteresis loop of the H3 type (IUPAC classification), which are characteristic of mesoporous materials. A characteristic sharp rise in the region of the nitrogen relative pressure p/p_0 above 0.9 indicates the presence of large mesopores (40–50 nm) and the smallest macropores (50–200 nm) in the structure, the filling of which is divided by a vertical line on the isotherms. MChT of natural CL, as well as its annealed forms, to one degree or another, increases its specific surface area and sorption volume of pores (Table 2) due to the development of mesoporosity and the growth of the volume of the above-mentioned macropores, as shown in work[32].

The H-form CL has a significantly higher specific surface area because a part of the cations is removed during acid treatment and a certain amount of micropores becomes available for nitrogen molecules during measurement (Table 2). The subsequent MChT reduces the specific surface area of acid-modified samples, but contributes to the increase of the sorption volume of pores (and its components), as well as for the original natural CL. For all undoped CL, MChT increases the content of macropores, the volume of which reaches 0.1–0.2 $cm^3 \cdot g^{-1}$.

As a result of MChT of natural CL in the presence of additives, a structure is formed, which is characterized, as a rule, by a smaller specific surface and a smaller sorption volume of pores compared to MChT of pure CL under similar conditions. At the same time, the specific surface area of the obtained doped samples is higher than that of the original natural CL. The hysteresis loops on the nitrogen adsorption-desorption isotherms of calcined and doped samples are more pronounced and located in a larger range of p/p_0 (Fig. 2, *b*), and on the curves of the distribution of pore volume by size for doped samples, there is a second, rather wide, maximum in the region of mesoporosity (Fig. 3). It can be seen that increasing the silver content causes this maximum to shift to a larger pore size. It is also important that for doped samples the contribution of mesopores to the sorption volume of pores is 60–70 %, while for undoped samples it is only 35–45 %. This redistribution of the pore volume is obviously caused by the introduction of metal oxide clusters into the CL structure, as well as the partial decomposition of nitrates, as a result of which additional mesoporosity can be generated accordingly to the so-called Pilling – Bradworth ratio.

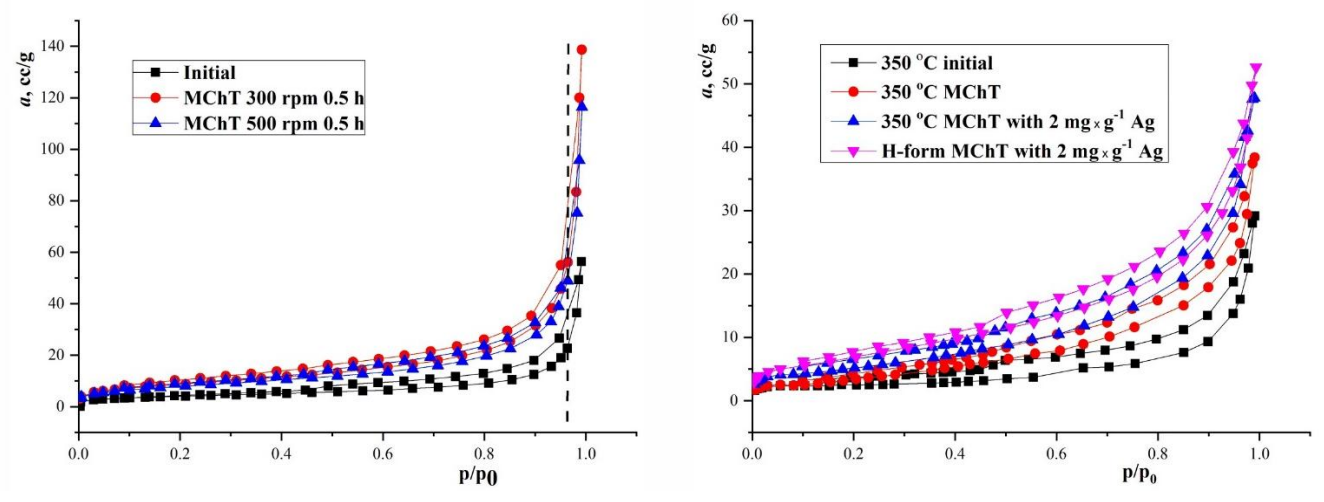

Fig. 2. Adsorption-desorption isotherms of nitrogen in natural CL before and after MChT **(a)**. Nitrogen adsorption-desorption isotherms for natural CL, annealed at 350 ºC and subjected to MChT with silver, as well as H-form with silver **(b)**

Table 2. Parameters of the porous structure of CL before and after MChT

No. sample	Form of CL	S, $m^2 \cdot g^{-1}$	V_s, $cm^3 \cdot g^{-1}$	V_{me}, $cm^3 \cdot g^{-1}$	V_{mi}, $cm^3 \cdot g^{-1}$	d, nm
	CL	14	0.085	0.035	–	4.2
1	*CL	32	0.215	0.080	0.005	3.7
7	*CL	35	0.350	0.350	–	5.8
8	*CL	30	0.110	0.110	–	3.6; 32
2	**CL	28	0.180	0.075	–	4.2
43	CL	29	0.09	0.09	–	4.3; 12.0
9	CL	18	0.075	0.075		4.0
42	CL	33	0.48	0.48	–	3.8; 17.1
41	CL	29	0.095	0.095	–	3.8
15	CL	26	0.065	0.065	–	3.9; 14.0
CL 350 ºC standard		10	0.045	0.045	–	3.7
21	CL	15	0.060	0.060	–	3.9
22	CL	17	0.075	0.075		4.0
47	CL	19	0.10	0.10	–	3.8; 32.0
13	CL	12	0.07	0.07	–	3.8
H-CL standard		73	0.120	0.045	0.020	3.8
4	H-CL	46	0.205	0.080	0.010	3.7
5	H-CL	32	0.265	0.085	–	3.7
45	H-CL	41	0.09	0.09	–	3.8; 12.2
20	H-CL	28	0.08	0.08	–	3.8
46	H-CL	45	0.11	0.11	–	4.0
18	Na-CL	20	0.13	0.13	–	3.8

* Samples 1, 7, 8 – rotation speed 300 rpm; duration of processing, respectively – 0.5, 1.5, 2.5 hours.
** Sample 2 – rotation speed 500 rpm; duration of processing – 0.5 h.

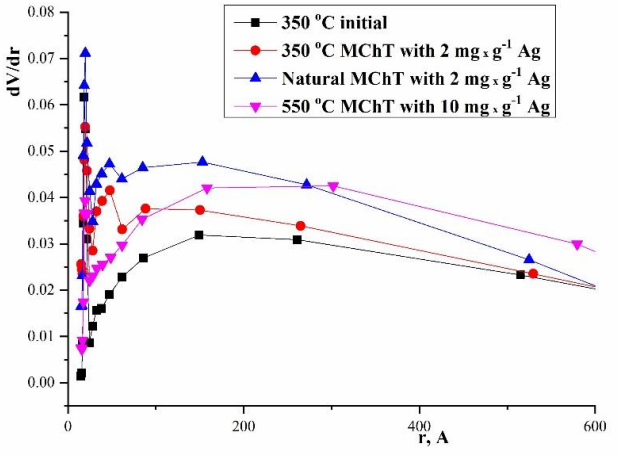

Fig. 3. The pore size distribution (PSD) curves for undoped and doped with silver samples

Thus, the regularities and features of the influence of dry MChT conditions, such as the intensity, duration, nature and content of the doping additive, on the parameters of the porous structure of the obtained samples of CL. On their basis, the optimal conditions were chosen, namely, the intensity – 400 rpm, the duration – 1 h. CL samples obtained in this way have a higher specific surface area compared to the original natural CL, as well as a better developed meso-macroporous structure, which contributes to increasing the accessibility of substrates to the active centers of the surface of CL particles.

3.2. Structural Characterization of CL Particles Using IR Spectroscopy

For CL, as well as for other zeolites, two groups of oscillations in the spectra are characteristic[30, 35]. Absorption bands (a.b.) associated with internal vibrations of Si–O(Si) and Si–O(Al) in tetrahedral or aluminum-silica bridges are in the range of 1200–400 cm^{-1}. In particular, the most important "zeolite" bands include asymmetric modes of valence vibrations of internal T–O bonds in TO_4 tetrahedra (T = Si and Al) (1045–1080 cm^{-1})[35].

Although the bands in the obtained spectra are rather wide, it can be established that the sp. 1062 cm^{-1} for the original natural CL is significantly expanded, and its maximum shifts to 1073 and 1074 cm^{-1} after dry MChT of natural CL at 300 and 500 rpm, respectively (Fig. 4, *a*). This may be related to the destruction of the aluminosilicate framework of the zeolite and the formation of additional siloxane bonds[36]. The enrichment of the surface with silica due to MChT is described in[32], based on the results of X-ray electron spectroscopy.

The bands, due to the presence of surface hydroxyl groups and zeolitic water, are in the range of 1600–3700 cm^{-1}. Thus, a.b. at 3650 cm^{-1} refers to valence vibrations of isolated OH groups, and the sp. at 3223 cm^{-1} to water sorbed in micropores[37]. The first band shifts to 3624 cm^{-1} after MChT, and the second one does not change its position, as does the band at 1630 cm^{-1}, which belongs to the deformation vibrations of hydroxyls in adsorbed water molecules.

The introduction of metals into the CL structure during MChT at 400 rpm causes even more significant changes in the spectra (Fig. 4, *b*). In order to compare the obtained spectra and identify changes in them depending on the MChT conditions, the spectra are presented in the coordinates of the Kubelka-Munk equation.

The spectra presented in Fig. 4, *b* characterize the structure of the surface of the obtained samples, in particular the surface OH groups. A significant increase in the absorption in this region due to MChT is visible, associated with an increase in specific surface area. In addition, a.b. caused by valence vibrations of various hydroxyl groups and forms of adsorbed water overlap, forming a very broad band in the region of 3800–2750 cm^{-1}. In particular, the band at 3615 cm^{-1}, responsible for the valence vibrations of the surface OH groups, can be traced in the spectrum of the silver-doped sample in the form of a shoulder (marked by a dash in Fig. 4, *b*). An increase in its intensity compared to the original sample is also clearly visible. Absorption bands responsible for deformational vibrations of OH groups in adsorbed water molecules shift from 1630 to 1645 cm^{-1}. At the same time, its intensity increases significantly, which also indicates an increase in surface hydroxylation as a result of doping by MChT.

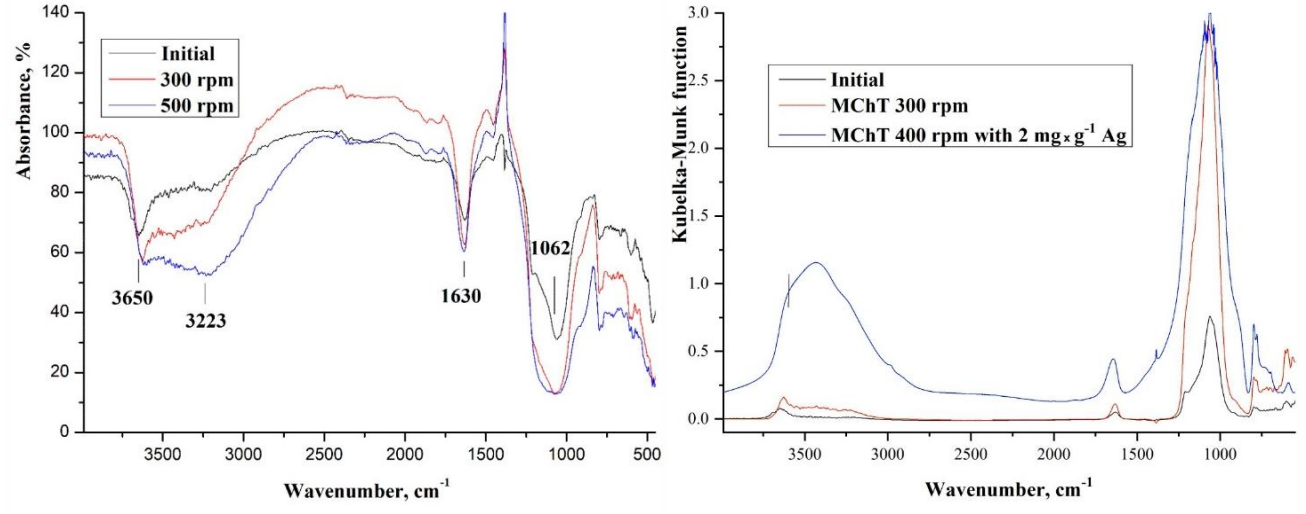

a b

Fig. 4. IR spectra of CL before and after MChT under different conditions (**a**). IR spectra in the interval 4000–1500 cm^{-1} of natural CL with silver additives before and after MChT (**b**)

Doping during MChT, carried out under different conditions, also leads to significant changes in the spectrum region, which refers to the vibrations of the Si–O–Al bonds of the clinoptilolite framework, namely, in the range of 1500–450 cm^{-1}. First of all, this applies to MChT at 400 rpm in the presence of silver additives (Fig. 4, *b*). Thus, a shift of the 1062 cm^{-1} band for the original natural CL to the values of 1070 cm^{-1} for the modified samples was detected, as well as an increase in the intensity of absorption in this region in comparison with the original sample. In addition, the spectrum of this sample shows an additional absorption band at 1095 cm^{-1}, apparently due to the introduction of silver into the aluminosilicate framework.

Thus, the results of IR spectroscopy indicate the formation of additional surface OH groups and siloxane bonds due to the partial destruction of the CL framework during MChT and an increase in its specific surface area. In addition, there is an introduction of silver into the CL matrix. The listed changes contribute to the formation of new active centers on the surface of the modified CL.

3.3. Electron Spectroscopy for Structural and Functional Characterization of CL Microparticles

Antimicrobial properties of materials, among other things, depend on their electronic characteristics[38, 39], since the latter determine the formation of reactive oxygen-

containing particles, including radicals (reactive oxygen species). In the electronic spectra of synthetic zeolites, no absorption in the range λ >300 nm was detected, while natural CL also absorbs visible radiation[40]. These features are due to the presence of impurities in its composition, primarily iron and titanium oxides[40, 41]. Indeed, the spectra of the original and mechanochemically modified natural CL contain a band in the region of 500–510 nm, marked by a line in Fig. 5. This band can be attributed to iron-oxide clusters (Fe-oxygen species), as noted in works[42].

The introduction of silver cations into the CL structure with ion exchange or MChT causes the appearance of an additional band between 400 and 500 nm in the spectra (Fig. 5). These bands can refer to different states of silver on the surface and in the CL matrix – both in cation exchange positions and in the form of metallic silver[43]. According to the literature data, silver can be found in zeolites, including CL, both in the metallic and ionic states[44]. The spectra show that silver in the doped samples is mainly in the Ag^{+} state, that is, it occupies cation-exchange positions, since there is no clearly expressed surface plasmon resonance (SPR) signal in the spectrum which is attributed to the presence of metallic silver[45].

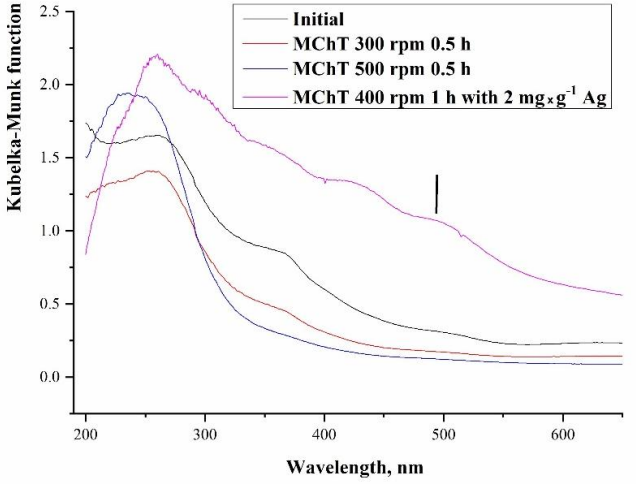

Fig. 5. Electronic spectra in the UV and visible region for natural CL before and after MChT under various conditions

The XPS spectra of Ag 3*d* electrons for the two silver-doped samples differ only in the intensity of the peaks, and the positions of Ag $3d_{3/2}$ and Ag $3d_{5/2}$ for both samples are almost the same – 374.4 and 368.5 eV, respectively (Fig. 6). It is known that the binding energies of 3*d* electrons for silver with different degrees of oxidation differ insignificantly, but the large width of the $3d_{5/2}$ peak indicates that silver is mainly in the form of Ag^{+46}.

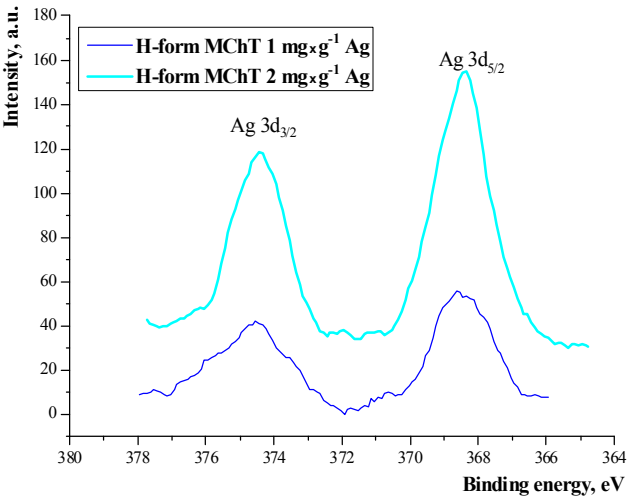

Fig. 6. XPS spectra of silver-doped CL

3.4. Antimicrobial Activity of CL Samples

Previously, it was established that unmodified CL has a relatively weak antibacterial activity. A certain correlation can be observed between the MChT conditions, on the one hand, and the antibacterial activity, on another hand: an increase in the intensity causes the formation of a more developed meso-macroporous structure, an increase in the available surface area and the content of hydroxyl and siloxane groups, which in turn contributes to a slight increase in activity. In general, thermal, chemical, and mechanical modifications of the CL structure increase the antibacterial activity, although the absence of an active agent in this structure does not allow us to fully establish these relationships[47]. Here, we improved the structure of CL to increase its ability to inhibit the growth and functioning of microorganisms by sorption of the transition metals, such as silver and copper, in various degrees of their oxidation, as well as *via* chemical treatment of the obtained CL samples.

In Fig. 7, the results of testing of the antibacterial activity of various CL samples are presented. Different species of bacteria were treated – Gram-positive bacteria – *Staphylococcus aureus, Bacillus subtilis,* and Gram-negative bacteria – *Pseudomonas aeruginosa*, *Pseudomonas fluorescence*. As can be seen from the results presented in Fig. 7, doping with silver significantly increases the antibacterial activity of CL samples. An unexpected feature turned out to be the dependence of antibacterial activity on the degree of oxidation, as we observed the decreasing level of antibacterial activity of the CL MPs dopped with the metallic silver (No. 43) or cuprum (No. 42), compared with such activity observed in the CL MPs dopped with the Ag cation (samples No. 9,

13, 22, 23, 24, 25, 39, 40, 47) or with Cu cation (samples No. 15, 26, 41).

One of the disadvantages of the use of silver-doped CL samples is their high cost. That is why we tested another metal for doping CL, namely copper. It was established that samples of CL doped with copper cation (Fig. 7, No. 15, 26, 31, 41) possessed antibacterial activity, which, in general, is comparable with the activity of samples of CL doped with silver cation.

To achieve higher antibacterial activity of CL samples doped with silver, they were modified with acid to obtain H- and Na-forms of CL. It was found that after sorption of silver on H- and Na-forms of CL (Fig. 8), a directly proportional relationship between the amount of silver and antibacterial activity was revealed only in H-forms of CL (samples No. 29–30). While an increase in the amount of silver sorbed on the Na-form of CL (samples No. 27–28) did not affect their antibacterial activity.

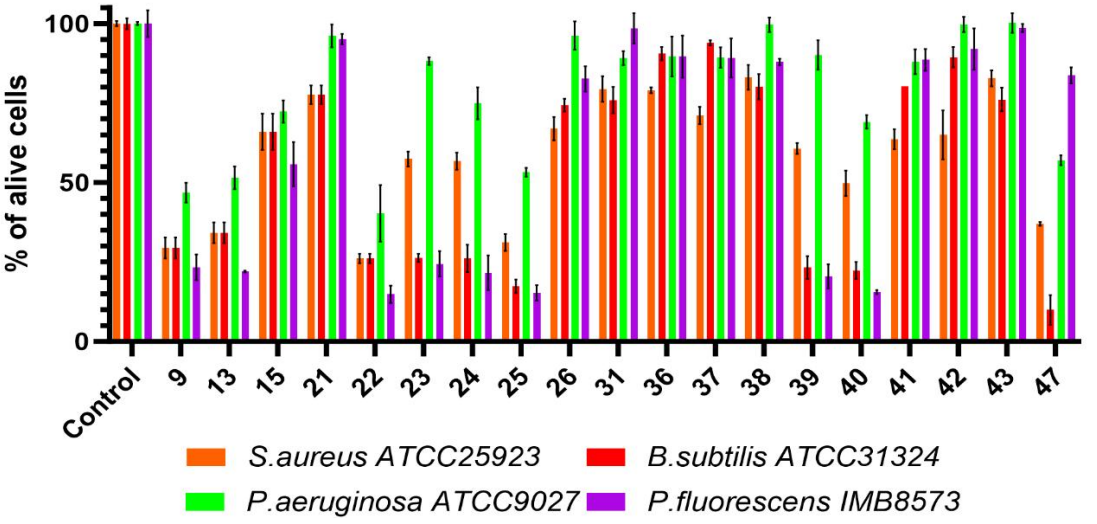

Fig. 7. Antibacterial activity of CL samples doped with silver MChT. The ordinate axis – percentage of alive cells, the abscissa axis – number of samples from Table 1,
Control – bacterial suspension without any agent

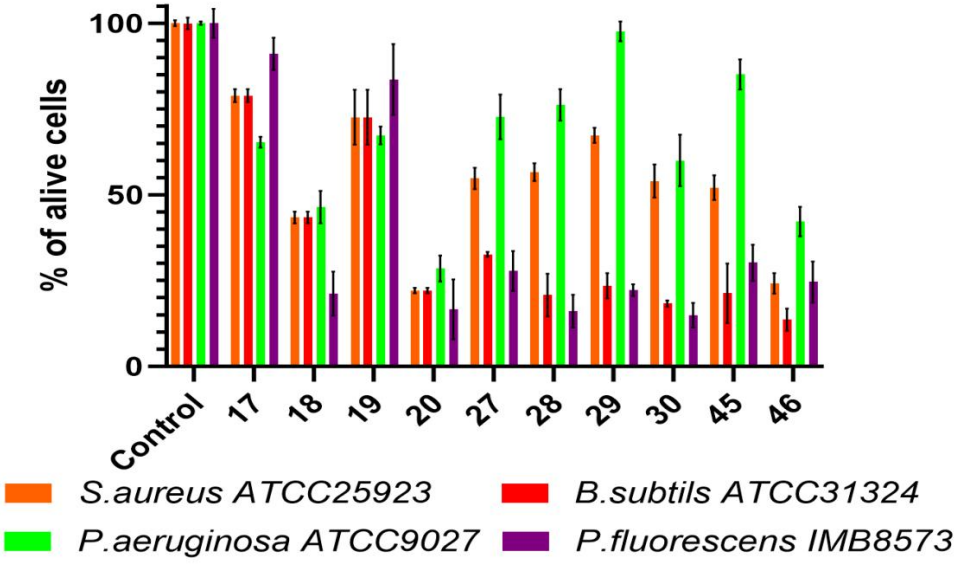

Fig. 8. Antibacterial activity of CL samples after metal sorption and MChT.
The ordinate axis – percentage of alive cells, the abscissa axis – number of samples from Table 1.
Control – bacterial suspension without any agent

After sorption of silver on the H-form of CL, a dependence of antimicrobial activity on the amount of silver in the sample was found only for *P. aeruginosa* bacteria. This may indicate a more efficient overcoming of the capsule barrier of these bacteria by the H-form CL with a higher amount of sorbed silver (6 mg of silver in sample No. 30, compared to 2 mg of silver in sample No. 29).

4. Conclusions

Novel MPs (0.8–50 micrometers) of the Transcarpathian CL were created *via* using various physicochemical treatments of these MPs based on their mechano-chemical, thermal, and chemical modifications, as well as *via* doping of the CL MPs with activator metals (Ag and Cu) of different degrees of oxidation. Structure-functional relationships (SAR) of created CL MPs were defined in the regards of their antimicrobial action towards Gram-negative (*Pseudomonas aeruginosa, Pseudomonas fluorescence)* and Gram-positive (*Staphylococcus aureus, Bacillus subtilis)* bacteria. **Type 1 of SAR**. The optimal conditions of MChT (400 rpm, 1 h, in air medium) were established for obtaining CL MPs with the required particle size, crystal structure, specific surface area, and porosity. MChT of all forms of CL MPs leads to its grinding (in some cases to amorphization) and the appearance of porosity, primarily due to the formation of additional meso- and macropores, and, as a result, to an increase in the specific surface. Such changes can facilitate better contact of CL with bacterial cells, while an increased content of larger pores improves their access to the active centers of the surface of the CL MPs. As a result of an increase in the specific surface area of CL MPs and partial destruction of the aluminosilicate frame, the content of active adsorption centers, such as additional hydroxyl groups and siloxane bonds, was increased. **Type 2 of SAR**. The inclusion of metals in the CL structure can promote the formation of active red-ox centers that might be responsible for the generation of reactive oxygen-containing particles participating in the destruction of bacterial cells. Silver cations significantly enhanced the antibacterial activity of CL, while a diminished activity was observed in samples of CL containing the metallic silver Ag(0). Similarly, the CL MPs containing metallic copper were less active, compared to the MPs containing Cu^{2+} cations. **Type 3 of SAR**. A directly proportional relationship was revealed between the amount of Ag^{+} in the doped samples of H-form CL MPs and their antibacterial activity. While an increase in the amount of Ag^{+} in the doped Na-form CL MPs did not influence their antibacterial activity. A difference between individual types of bacteria was revealed in terms of the effects of some samples of CL. The amount of Cu^{2+} in the CL MPs did not significantly affect their antibacterial activity. **Type 4 of SAR**. It is not only the structure of the CL MPs that affects their antibacterial action, but the morphology of the bacterial cells can also modify such action. It was found that the presence of polysaccharide capsule covering *P. aeruginosa* cells significantly reduced the antibacterial activity of the CL samples. On the other hand, peptidoglycan released into the environment by *B. subtilis* bacteria does not significantly affect the antibacterial effect of CL samples doped with silver, which allows us to assume the possible effectiveness of CL against bacterial contamination or biofilms. Thus, the antimicrobial activity of CL can be enhanced using various physico-chemical modifications of its MPs, and different SARs exist for realizing such effects.

Acknowledgements

The authors acknowledge the Rota Mining Corporation for supplying the natural clinoptilolite zeolite.

This work was carried out as part of the NRFU project N 2022.01/0105, State registration number: 0123U103586, “New means based on compositions of natural zeolite for disinfection of surfaces in the field conditions”.

The authors acknowledge the Microorganisms Collection of Biololgy Faculty of Ivan Franko National University for providing strains for antimicrobial research.

Abbreviations

CL – Transcarpathian clinoptilolite.

References

[1] Blazheyevskiy, M. Ye.; Riabko, D. N. *Application of peroxy acids as disinfectants and sterilization agents (monograph)*; LAP LAMBERT Academic Publishing, 2014.

[2] Jang, Y. J.; Kim, K.; Tsay, O. G.; Atwood, D. A.; Churchill, D. G. Destruction and Detection of Chemical Warfare Agents. *Chem. Rew.* **2015**, *115*, PR1–PR76. https://doi.org/10.1021/acs.chemrev.5b00402

[3] Tušek, D.; Ašperger, D.; Bačić, I.; Ćurković, L.; Macan, J. Environmentally Acceptable Sorbents of Chemical Warfare Agent Simulants. *J. Mater. Sci.* **2017**, *52*, 2591–2604. https://doi.org/10.1007/s10853-016-0552-x

[4] Singh, V. V.; Jurado-Sánchez, B.; Sattayasamitsathit, S.; Orozco, J.; Li, J.; Galarnyk, M.; Fedorak, Yu.; Wang, J. Multifunctional Silver Exchanged Zeolite Micromotors for Catalytic Detoxification of Chemical and Biological Threats. *Adv. Funct. Mater.* **2015**, *25*, 2147–2155. https://doi.org/10.1002/adfm.201500033

[5] Znak, Z.; Kochubei, V. Influence of Natural Clinoptilolite Modification with Ions and Zero-Valent Silver on Its Sorption Capacity. *Chem. Chem. Technol.* **2023**, *17*, 646–654. https://doi.org/10.23939/chcht17.03.646

[6] Voloshyna, Y.; Pertko, O.; Povazhnyi, V.; Patrylak, L.; Yakovenko, A. Effect of Modifying the Clinoptilolite-Containing Rocks of Transcarpathia on Their Porous Characteristics and Catalytic Properties in the Conversion of C6-Hydrocarbons. *Chem. Chem. Technol.* **2023**, *17*, 373–385. https://doi.org/10.23939/chcht17.02.373
[7] Kraljević Pavelić, S.; Simović Medica, J.; Gumbarević, D.; Filošević Vujnović, A.; Przuljet N.; Pavelićal, K. Critical Review on Zeolite Clinoptilolite Safety and Medical Applications *in vivo*. *Front Pharmacol.* [Online] **2018**, *9*, 1350. https//doi.org/10.3389/fphar.2018.01350
[8] Rainer, D. N.; Morris, R. E. New Avenues for Mechano Chemistry in Zeolite Science. *Dalton Trans.* **2021**, *50*, 8995–9009. https://doi.org/10.1039/d1dt01440d
[9] Gatta, G.; Lotti, D., Systematics, Crystal Structures, and Occurrences of Zeolites. In *Modified Clay and Zeolite Nanocomposite Materials*. *Environmental and Pharmaceutical Applications*, 2019, pp. 1–25. Tarasevich, Yu. I. *Surface Phenomena on Disperse Materials*, Naukova dumka: Kyiv, 2011.
[10] EFSA Panel on Additives and Products or Substances used in Animal Feed (FEEDAP). Scientific Opinion on the safety and efficacy of clinoptilolite of sedimentary origin for all animal species. *EFSA J.* [Online] **2013**, *11*, 3039. https://doi.org/10.2903/j.efsa.2013.3039
[11] Kahramanova, X. T.; Sadikhova, F. E.; Veliyeva, M. N.; Kahramanova, X. T.; Ibadova, X. I. Zeolite is Biologically Active Mineral. In *Natural Zeolite in Medicine*; SWB, 2010; pp 10–35.
[12] Flowers, J. L.; Lonky, S. A.; Deitsch, E. J. Clinical Evidence Supporting the Use of an Activated Clinoptilolite Suspension as an Agent to Increase Urinary Excretion of Toxic Heavy Metals. *Diet. Suppl.* [Online] **2009**, *1*, 11–18. https://doi.org/10.2174/NDS.S8043
[13] Vasylechko, V. O.; Fedorenko, V. O.; Gromyko, O. M.; Gryshchouk, G. V.; Kalychak, Ya. M.; Zaporozhets, O. A.; Lototska, M. T. Solid Phase Extractive Preconcentration of Silver from Aqueous Samples and Antimicrobial Properties of the Clinoptilolite–Ag Composite. *Adsorpt. Sci. Technol.* **2017**, *35*, 602–611. https://doi.org/10.1177/0263617417703509
[14] Vasylechko, V. O.; Fedorenko, V. O.; Gromyko, O. M.; Gryshchouk, G. V.; Kalychak, Y. M.; Tistechok S. I.; Us, I. L.; Tupys, A. Sorption Preconcentration of Silver for Atomic Absorption Analysis and Antibacterial Properties of the Acid-modified Clinoptilolite – Ag composite. Methods. *Objects Chem. Anal.* **2020**, *15*, 73–82. https:/doi.org/10.17721/moca.2020.73-82
[15] Vasylechko, V.; Fedorenko, V.; Gromyko, O.; Gryshchouk, G.; Kalychak, Ya.; Tistechok S.; Us, I.; Tupys, A. A Novel Solid-Phase Extraction Method for Preconcentration of Silver and Antimicrobial Properties of the Na-clinoptilolite–Ag Composite. *Mater. Today: Proc.* **2021**, *35*, 548–551. https://doi.org/10.1016/j.matpr.2019.10.049
[16] Patrylak, L. K.; Yakovenko, A. V.; Nizhnik, B. O.; Pertko, O. P.; Povazhnyi, V. A.; Kamenskyh, D. S.; Melnychuk, O. V. Natural Zeolites Modified with Silver Nanoparticles as Promising Sorbents with Antibacterial Properties. Nanoelectronics, Nanooptics, Nanochemistry and Nanobiotechnology, and Their Applications. NANO 2022. Springer Proceedings in Physics. Springer, Cham. **2023**, *297*, 87–98. https://doi.org/10.1007/978-3-031-42708-4_5
[17] Gromyko, O. M.; Vasylechko, V. O.; Gryshchouk, G. V.; Roman, I. I.; Kalychak, Ya. M.; Fedorenko, V. O.; Bagday, S. R. Antimicrobial Activity of Transcarpathian Clinoptilolite Modified with Salts of Transition Metals. Book of Abstracts of International research and practice conference "Nanotechnology and nanomaterials" (NANO-2022). Lviv, Ukraine. Kyiv: LLC APF POLYGRAPH SERVICE, 2022.
[18] Rossainz-Castro, L. G.; De-La-Rosa-Gómez, I.; Olguín, M. T.; Alcántara-Díaz, D. Comparison between Silver and Copper-Modified Zeolite-Rich Tuffs as Microbicide Agents for *Escherichia coli* and *Candida albicans*. *J. Environ. Manage.* **2016**, *183*, 763–770. https://doi.org/10.1016/j.jenvman.2016.09.034
[19] Milenkovic, J.; Hrenovic, J.; Matijasevic, D.; Niksic M.; Rajicet N. Bactericidal Activity of Cu-, Zn-, and Ag-Containing Zeolites toward *Escherichia coli* Isolates. *Environ. Sci. Pollut. Res.* **2017**, *24*, 20273–20281. https://doi.org/10.1007/s11356-017-9643-8
[20] Vasylechko, V. O.; Klyuchivska, O. Yu.; Manko, N. O.; Gryshchouk, G. V.; Kalychak, Ya. M.; Zhmurko, I. I.; Stoika, R. S. Novel Nanocomposite Materials of Silver – Exchanged Clinoptilolite with pre-Concentration of $Ag(NH_3)_2^+$ in Water Possess Enhanced Anticancer Action. *Appl. Nanosci.* **2020**, *10*, 4869–4878. https:/doi.org/10.1007/s13204-020-01353-7
[21] Paryzhak, S. Ya.; Dumych, T. I.; Klyuchivska, O. Yu. Manko, N. O.; Gryshchouk, G. V.; Vasylechko V. O.; Stoika R. S. Silver Doping of Clinoptilolite Particles Enhances their Effects on Immunocompetent Mammalian Cells and Inhibition of *Candida albicans* Fungi. *Appl. Nanosci.* **2023**, *13*, 4817–4826. https://doi.org/10.1007/s13204-022-02624-1
[22] Lemire, J. A.; Harrison, J. J.; Turner, R. J Antimicrobial Activity of Metals: Mechanisms, Molecular Targets and Applications. *Nature Rev. Microbiol*. **2013**, *11*, 371–384. https://doi.org/10.1038/nrmicro3028
[23] Tarasevich, Y. I.; Polyakov, V. E.; Penchov, V. Z. Ion-Exchange Qualities and Structural Features of Clinoptilolites of Various Deposits. *Khim. Tekhnol. Vody* **1991**, *13*, 132–140.
[24] Vasylechko, V. O.; Cryshchouk, G. V.; Lebedynets, L. O.; Kuz'ma, Yu. B.; Vasylechko, L. O.; Zakordonskiy, V. P. Adsorption of Copper on Transcarpathian Clinoptilolite. *Adsorp. Sci. Technol*. **1999**, *17*, 125–134. https://doi.org/10.1177/026361749901700206
[25] Vasylechko, V. O.; Gryshchouk, G. V.; Kaminska, M. I.; Stel'makhovych, B. M. A Solid-Phase Extraction Method Using Acid-Modified Transcarpathian Clinoptilolite for Preconcentration of Trace Amounts of Lead in Water Samples. *Appl. Nanosci.* **2019**, *9*, 1057–1065. https://doi.org/10.1007/s13204-018-0858-x
[26] Tarasevich, Y. I.; Polyakova, I.G.; Polyakov, V. E. Microcalorimetric Study of the Interaction of Water with Cation-Substituted Forms of Clinoptilolite. *J. Colloid Sci.* **2003**, *65*, 493–499. https://doi.org/10.1023/A:1025133221812
[27] Słota, E.; Vasylechko, V.; Patsay, I.; Gołębiowski, A.; Sprynskyy, M.; Buszewski, B.; Poddubnaya, O.; Puziy, A. The Use of H-Form Clinoptilolite to Preconcentrate Trace Amounts of Nd(III) from Aqueous Solution under Dynamic Conditions. *Micropor. Mesopor. Mater.* [Online] **2022**, *333*, 111739. https://doi.org/10.1016/j.micromeso.2022.111739
[28] Akselrud, L.; Grin, Y. *WinCSD*: software Package for Crystallographic Calculations. *J. Appl. Crystallogr.* **2014**, *47*, 803–805. https://doi.org/10.1107/S1600576714001058
[29] Korkuna, O.; Leboda, R.; Skubiszewska-Zięba, J.; Vrublevs'ka, T.; Gun'ko, V.; Ryczkowski, J. Structural and Physicochemical Properties of Natural Zeolites: Clinoptilolite and Mordenite. *Micropor. Mesopor. Mater.* **2006**, *87*, 243–254. https://doi.org/10.1016/j.micromeso.2005.08.002
[30] Sydorchuk, V.; Poddubnaya, O.; Tsyba, M.; Zakutevskyy, O.; Khyzhun, O.; Khalameida, S.; Puziy, A. Activated Carbons with Adsorbed Cations as Photocatalysts for Pollutants Degradation in Aqueous Medium. *Adsorption* **2019**, *25*, 267–278. https://doi.org/10.1007/s10450-018-00006-0

[31] Sydorchuk, V.; Vasylechko, V.; Khyzhun, O.; Gryshchouk, G.; Khalameida, S.; Vasylechko, L. Effect of High-Energy Milling on the Structure, Some Physicochemical and Photocatalytic Properties of Clinoptilolite. *Appl. Catal. A Gen.* [Online] **2021**, *610*, 117930. https://doi.org/10.1016/j.apcata.2020.117930
[32] Armbruster, T. Clinoptilolite – heulandide: applications and basic research.In *Zeolites and mesoporous materials at the down of the 21ST century. Studies in Surfase Science and Catalysis.* Vol. 135, Part C; Elsevier, 2001; pp 13–27.
[33] Zakordonskiy, V.; Vasylechko, V.; Staszczuk, P.; Gryshchouk, G. Water Thermodesorption and Adsorption Properties of the Transcarpathian Zeolites. *Visnyk Lviv Univ. Ser. Chem.* **2004**, *44*, 247–256.
[34] Elaiopoulos, K.; Perraki, T.; Grigoropoulou, E. Monitoring the Effect of Hydrothermal Treatments on the Structure of a Natural Zeolite through a Combined XRD, FTIR, XRF, SEM and N_2-Porosimetry Analysis. *Micropor. Mesopor. Mater.* **2010**, *134*, 29–43. https://doi.org/10.1016/j.micromeso.2010.05.004
[35] Innocenzi, P. Infrared Spectroscopy of Sol-Gel Derived Silica-Based Films. *J. Non-Crystalline Solids.* **2003**, *316*, 309–319. https://doi.org/10.1016/S0022-3093(02)01637-X
[36] Skubiszewska-Zieba, J.; Khalameida, S.; Sydorchuk, V. Comparison of Surface Properties of Silica Xero- and Hydrogels Hydrothermally Modified Using Mechanochemical, Microwave and Classical Methods. *Colloids and Surf. A.* **2016**, *504*, 139–153. https://doi.org/10.1016/j.colsurfa.2016.05.066
[37] Stanić, V.; Tanasković, S. B. Antibacterial Activity of Metal Oxide Nanoparticle. *Nanotoxicity* **2020**, 241–274. https://doi.org/10.1016/b978-0-12-819943-5.00011-7
[38] Khan, M. M.; Matussin, S. N.; Rahman, A. Recent Development of Metal Oxides and Chalcogenides as Antimicrobial Agents. *Bioprocess Biosyst. Eng.* **2023**, *46*, 231–1249. https://doi.org/10.1007/s00449-023-02878-1
[39] Alvarez-Aguiañaga, E. A.; Elizalde-González, M. P.; Sabinas-Hernández, S. A. Unpredicted Photocatalytic Activity of Clinoptilolite-Mordenite Natural Zeolite. *RSC Advances* **2020**, *10*, 39251–39260. https://doi.org/10.1039/D0RA06421A
[40] Pavlović, J.; Šuligoj, A.; Opresnik, M.; Novak Tušar, N.; Zabukovec Logar, N.; Rajić, N. Studies of Clinoptilolite-Rich Zeolitic Tuffs from Different Regions and their Activity in Photodegradation of Methylene Blue. *Catalysts* **2022**, *12*, 224. https://doi.org/10.3390/catal12020224
[41] Tong, Y.; Zhang, Y.; Tong, N.; Zhang, Z.; Wang, Y.; Zhang, X.; Zhu, S.; Li F.; Wang, X. HZSM-5 Zeolites Containing Impurity Iron Species for the Photocatalytic Reduction of CO_2 with H_2O. *Catal. Sci. Technol.* **2016**, 7579–7585. https://doi.org/10.1039/c6cy01237j
[42] Concepción-Rosabal, B.; Rodríguez-Fuentes, G.; Bogdanchikova, N.; Bosch, P. Comparative Study of Natural and Synthetic Clinoptilolites Containing Silver in Different States. *Micropor. Mesopor. Mater.* **2005,** *86*, 249–255. https://doi.org/10.1016/j.micromeso.2005.07.027
[43] Mintcheva, N.; Panayotova, M.; Gicheva, G.; Gemishev, O.; Tyuliev, G. Effect of Exchangeable Ins in Natural and Modified Zeolites on Ag Content, Ag Nanoparticle Formation and their Antibacterial Activity. *Materials* **2021**, *14*, 4153. https://doi.org/10.3390/ ma14154153
[44] Fang, M.; Tan, X.; Liu, Z.; Hu, B.; Wang, X.; Recent Progress on Metal-Enhanced Photocatalysis: A Review on the Mechanism. *Research* [Online] **2021**, ID:9794329. https://doi.org/10.34133/2021/9794329
[45] Hoflund, G. B.; Hazos, Z. F.; Salaita, G. N. Surface Characterization Study of Ag, AgO, and Ag_2O Using X-Ray Photoelectron Spectroscopy and Electron Energy-Loss Spectroscopy. *Phys. Rev. B.* **2000**, *62*, 11126. https://doi.org/10.1103/PhysRevB.62.11126
[46] Manko, N. O.; Vasylechko, V. O.; Kostiv, O. I.; Kluchivska, O. Yu.; Sydorchuk, V. V., Ilkov, O. O.; Bagday, S. R.; Zelinskiy, A. V.; Gromyko, O. M.; Kalychak, Ya. M.; *et al*. Study of Antibacterial Effects of Transcarpathian Clinoptilolite Compositions Modified by Different Chemical Ways. *Studia Biologica* **2024**, *18*, 3–17. https://doi.org/10.30970/sbi.1802.767

Received: June 04, 2024 / Revised: October 20, 2024 / Accepted: Novembrer 18, 2024

ВПЛИВ ФІЗИКО-ХІМІЧНОЇ МОДИФІКАЦІЇ КЛИНОПТИЛОЛІТОВИХ КОМПОЗИТІВ НА ЇХНЮ АНТИМІКРОБНУ АКТИВНІСТЬ

Анотація. *Мікрочастинки на основі природного закарпатського клиноптилоліту (КЛ), його H- та Na-форм синтезовані фізико-хімічними модифікаціями, зокрема, термічною обробкою та допуванням металами-активаторами (Ag та Cu). Допування зразків КЛ іонами металів здійснено двома різними способами: перший полягав у використанні методу твердофазної екстракції в динамічних умовах із подальшим застосуванням механо-хімічної обробки, другий – у механо-хімічній обробці зразків КЛ зі сполуками Ag і Cu. Досліджено XRD, SEM, EDX, FTIR-, UV-Vis-, XPS спектри, дисперсність, параметри пористої структури й антибактеріальну активність отриманих композицій. Модифіковані форми характеризуються підвищеною дисперсністю, більшою площею питомої поверхні, пористістю. Включення металів у структуру КЛ сприяло формуванню активних red-ox центрів, відповідальних за утворення активних кисневмісних частинок, які беруть участь у руйнуванні мікроорганізмів, що істотно підвищує антибактеріальну активність КЛ. Фізична стабільність і біотолерантність КЛ у поєднанні із запропонованими підходами фізико-хімічної модифікації цеоліту будуть корисними для приготування нових засобів для дезінфекції забруднених поверхонь у промисловості, сільському господарстві тощо.*

Ключові слова: *клиноптилоліт, мікрочастинки, перехідні метали, фізико-хімічні та механохімічні модифікації, антимікробна дія.*